MATERIALS PHYSICS AND MECHANICS RESEARCH ARTICLE

Submitted: April 10, 2025 **Revised: June 23, 2025** **Accepted: July 22, 2025**

Evaluating the impact of functionalized graphene integration on thermal properties of CFRP composites

D.N. Choudhury [1,2] ✉, **S.K. Panda** [1]

[1] Indian Institute of Technology (BHU) Varanasi, Varanasi, India

[2] Aircraft Research & Design Center, HAL, Bangalore, India

✉ debendranchoudhury.rs.mec18@itbhu.ac.in

ABSTRACT

This study highlights the improvement in the thermal properties of CFRP composites modified with lower concentrations of graphene reinforcement (ADG-NH_2/epoxy/CFRP). Thermal properties such as storage modulus, loss modulus, damping factor and glass transition temperature of the composites were investigated through dynamic mechanical analysis with a temperature scan range of 30 to 200 °C and thermogravimetric analysis measurements. Five symmetrical CFRP composite laminates were prepared through a hand layup process assisted by vacuum bagging technique using various wt. % proportions (0.25, 0.5, 0.75 and 1) of ADG-NH_2/epoxy along with a neat epoxy. A slight increase of ~ 2 % in the glass transition temperature T_g was observed for the modified composites. It was observed that the ADG-NH2 composites showed ~54 % increment in storage modulus E', ~ 41 % increase in loss modulus E'' compared to neat epoxy CFRP laminate composites. Thermal stability values were determined through integral procedural decomposition temperature measurement and an enhancement from 389.1 to 411.9 °C was observed. Morphological properties of fracture surfaces were characterized by SEM micrographs and XRD analysis.

KEYWORDS

composite • CFRP • amine functionalized graphene • DMA • TGA • SEM • XRD

Citation: Choudhury DN, Panda SK. Evaluating the impact of functionalized graphene integration on thermal properties of CFRP composites. *Materials Physics and Mechanics*. 2025;53(3): 122–139. http://dx.doi.org/10.18149/MPM.5332025_10

Introduction

Many engineering and industrial applications have broadened the requirement for carbon fiber-reinforced polymer (CFRP) composites because of their superior thermal properties such as stability, high insulation, high heat resistance, low shrinkage along with enhanced mechanical properties like good dimensional stability, high tensile strength and modulus etc. [1–5]. Nano additives like 2-D Graphene sheet composed of honeycomb structure arrangement SP^2 carbon atoms were used in CFRP structures to enhance mechanical, electrical and thermal properties [6,7]. Covalent functionalization shows more variation in material properties and excellent bonding between the functional groups and particle surfaces. Covalent bonding between the matrix and additive enables enhanced electric charge, phonons transfer as well as mechanical load transfer across the particle / polymer interface [8–11]. In order to form a strong amide bond with epoxies, amine functionalities take part in the polymerization process [12] which is cured with amine-based hardeners and are used in the majority of structural FRPs.

Many literatures report the study of crystallization behavior of polymeric composites with the addition of very small amounts of graphene nano particles through

non-isothermal DSC experiment analysis [13]. Through thermogravimetric analysis (TGA) measurements, thermal degradation and thermal stability characteristics of polymeric composites subjected to higher thermal loading and high temperature resistance to mechanical deformations were investigated [14,15]. The viscoelastic properties of the polymeric composites subjected to continuous sinusoidal loads such as damping factor (tan δ), storage modulus (E') and loss modulus (E'') were analyzed through dynamic mechanical analysis (DMA) [16,17]. Storage modulus (E') indicates the rigidity and stiffness of the polymeric structure and decreases with increase in temperature due to the movement of polymeric chain segments [18,19]. Heat-released energy with the viscous reaction of the composite was analysed by the measure of Loss modulus (E''). The ratio of storage modulus (E') to loss modulus (E'') was measured by damping factor (tan δ) [20,21].

Numerous studies have validated that combining synthetic fibers with plant-based fibers can enhance the viscoelastic properties of composite materials [22–24]. A high concentration of carbon-based materials has been shown to enhance the thermal conductivity of polyamide composites. In a separate study, the thermal behavior of epoxy resin-based composites was investigated by incorporating varying concentrations of graphene nanoplatelets (GNPs) - specifically 0.25, 0.5, and 0.75 wt. % - using ultrasonic dispersion. The findings revealed that the composite containing 0.75 wt. % GNPs exhibited superior thermal stability compared to the other formulations [25]. It is reported that the crystallization temperature and degree of crystallinity of polyamide graphene nanoplatelet (GNP) nanocomposites increase with higher graphene loading [26]. Rheological analysis further revealed that increasing the GNP weight percentage enhances both the storage modulus and complex viscosity of the material. At elevated graphene concentrations, a low-frequency plateau was observed, indicating a pseudo-solid-like behavior in the polymer melt. Recent studies have shown that graphene nanoplatelets (GNPs), particularly those prepared through acid treatment for improved suspension stability, significantly enhance the thermal conductivity and stability of polymer composites. When these heat-exfoliated graphene layers are embedded into epoxy matrices, they yield notable improvements in thermal performance [27]. In another study, it has been shown that functionalized graphene oxide (GO)-reacted with agents such as Ceylon achieved a thermal conductivity of up to 5.8 W/m·K with 20 wt. % GO loading. Under mechanical stress, GO-based polymer composites demonstrated a higher tendency to form well-dispersed nanostructures, resulting in significantly improved thermal conductivity [28].

From the existing literature, it was observed that less work has been carried out on the thermal properties of CFRP composites reinforced with low content graphene nano particles ($\leqslant$ 1.0 wt. %) compared to high-content graphene-filled polymer composites. This paper reports on the preparation of amine-functionalized graphene-epoxy CFRP composites with different percentages of ADG-NH_2 loading ($\leqslant$ 1 wt. %) and investigation of thermal properties and morphological properties to establish the effect of amine functionalization on the CFRP composites. This paper also describes the processing method of ADG-NH_2 into the epoxy matrix, which has enhanced the properties due to the better homogeneous dispersion of the ADG-NH_2. The main highlights of the research work are use of aerospace grade epoxy and resin with amine functionalized graphene. Significant increase in the storage modulus and loss modulus at 0.5 wt. % of ADG-NH_2 graphene content compared to the neat epoxy CFRP composites indicating better

elasticity, viscoelastic properties and energy dissipation capabilities. Minimum tan δ for 0.5 wt. % of ADG-NH_2 graphene content compared to neat epoxy indicating better damping, energy dissipation and superior interfacial bonding between fiber and matrix interface. Fractographic analysis from scanning electron microscopy (SEM) and X-ray diffraction (XRD) clearly demonstrates the improvement of layer adhesion for increasing loading content up to compared to neat epoxy CFRP.

Materials

The amine functionalized graphene (product No.: ADG-NH_2) was received from M/s AdNano Technologies Private Limited, Shivamogga, Karnataka, India. Homogeneous dispersion (purity ~ 99 %) of the amine functionalized graphene (containing 5–10 layers of graphene) with the addition of (~ 2 to 5 %) NH_2 to graphene in order to achieve the desired exfoliation and dispersion increases the thermal conductivity and mechanical properties. The covalently functionalized graphene particles have an average thickness range of 5–10 nm and an average lateral dimension of the range 5–10 µm with bulk density and surface area of 0.1 g/cm^3 and 60-200 m^2/g, respectively (Fig. 1).

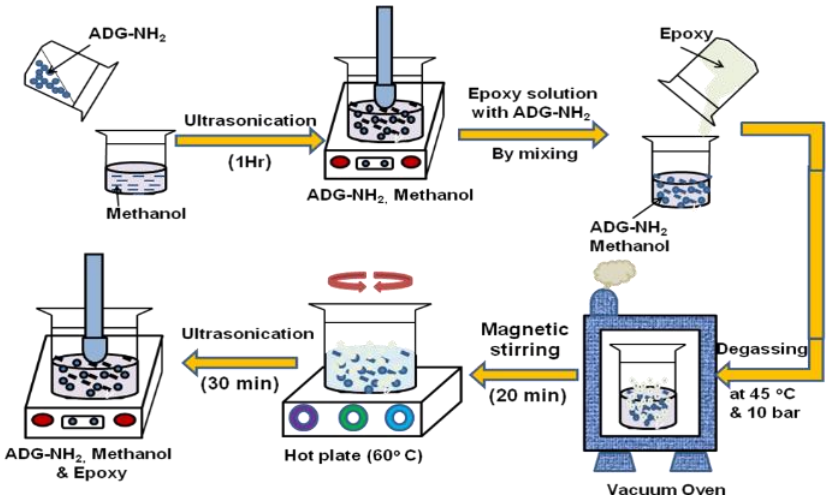

(a)

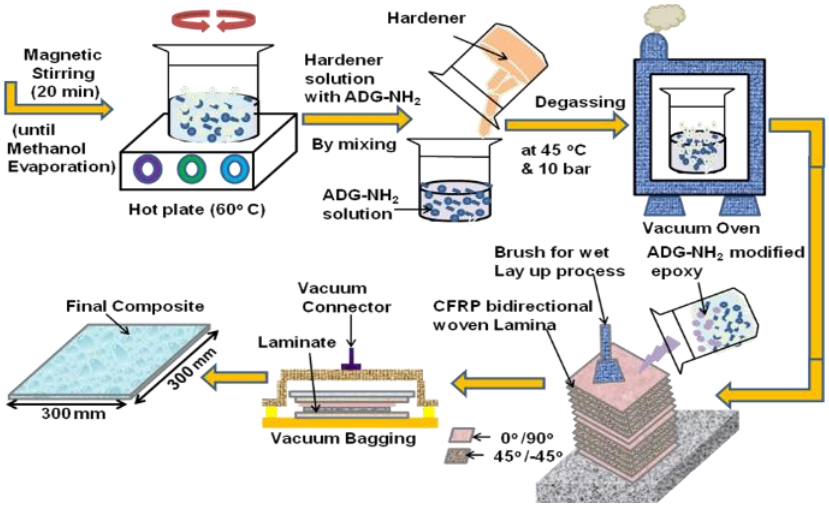

(b)

Fig. 1. Schematic diagram of processing of ADG-NH_2 (a) and (b) fabrication of laminated components

Bidirectional carbon fiber woven fabrics (T700), epoxy (LY 5052) and hardener (CH 5052) were used for this study. The high-strength non-crimp carbon fiber fabrics (Product No.: T700) were purchased from M/s Carbonext India Private Limited. Nashik, Maharashtra, India has a thickness of 0.25 mm or 250 gsm. The T700 carbon fiber fabric had an aerial weight of 634 g/m^2 (305 g/m^2 in the 90° direction, 315 g/m^2 in the 0° direction and was stitched together with polyester knitting thread (14 g/m^2). An aerospace-grade epoxy resin (ARALDITE LY5052) and hardener (ARADUR 5052 CH) received from M/s Singhal Chemical corporation, Meerut, UP, India were used for this study. The resin was mixed with hardener with a ratio of 100:38 (wt. %). Initially a baseline T700 carbon fiber fabric CFRP composite with neat epoxy was manufactured. The mould release agent was received from Mohini Organics Pvt. Ltd., Malad (West), Mumbai, Maharastra, India and adhesive tape, release film & peel ply were purchased from Aristo Flexi pack, Daman and Diu, India. For this composite Laminate system, the densities of fiber and resin are 1.8 and 1.17 g/cm^3 respectively and the nominal resin and fiber volume was of the ratio 34: 66.

Fabrication of amine functionalized graphene (ADG-NH_2)/epoxy

As shown in schematic representation (Fig. 1), during this study all the composite laminates were prepared under similar environmental conditions. The desired amine functionalized graphene (ADG-NH_2) solution loading content was added to solvent medium (methanol) and dispersed using an ultrasonic dispersion machine (Hielscher Ultrasonic homogenizer (Product No. UP400 ST) with a 22 mm probe), for 1 h to ensure the homogeneous dispersion of ADG-NH_2 by breaking the Vander walls attractive force of attraction between the nano particles. This process completely removes ADG-NH_2 aggregates, enabling effective dispersion. A large volume of methanol solvent was used for dispersion of ADG-NH_2. The base epoxy resin was then added to the ADG-NH_2/methanol dispersion and the mixture was stirred continuously with a magnetic stirrer. Methanol was evaporated from the ADG-NH_2-epoxy solution by using a rotorvap machine which was operated at 45 °C (10 bar). The resulting mixture was then allowed to settle down inside the oven at 45 °C under the vacuum at 10 bar and methanol was completely evaporated. A mixing machine with high speed of rotation (ROSS Laboratory High shear mixer (Model 100LH), NY USA) operating at 3000 rpm for 20 min was used to mix the ADG-NH_2/epoxy. The mixtures were then allowed to settle down on the beaker stand and the agglomerates were completely removed. The neat epoxy was treated similarly as the processing stage of ADG-NH_2 different wt. % filler loadings [29,30]. Hardener Aradur 5052 CH was then added to the ADG-NH_2/ epoxy solution and a mixing ratio of 100:38 was incorporated, which was mixed again using the mixing machine with high speed of rotation at 3000 RPM for 20 min. Then the degassing of the suspension was carried out in a vacuum chamber (pressure ~ 10 bar) at 45 °C for approximately 20 min while manual mixing through a mechanical stirrer was carried out during the entire process. The mixture was then transferred into an open beaker at room temperature (RT), which was used for the preparation of the CFRP laminate.

Fabrication of composite laminates

Bidirectional carbon fiber was cut into 4 pieces of 300 × 300 mm^2 with 0°/90° orientation and 8 pieces of 45°/-45° orientation to prepare CFRP Laminate. For fabrication of the

laminate, a 15 mm thick plane aluminum plate was considered, and its top face was cleaned thoroughly with MEK on which the laminate wet lay-up process was carried out. A release film (300 × 300 mm^2) with 15 μm thickness was laid and on it a peel ply (30 μm) was laid. With the help of a brush, the mould release agent was applied to the peel ply and prepared adhesive resin solution (ADG-NH_2+ epoxy (LY 5052) + Hardener (5052 CH)) was applied on it. Then the first carbon fiber bidirectional woven sheet (in 0°/90° orientation) was kept on the adhesive resin solution. Then the second carbon fiber layer (at 45°/-45° orientation) was kept over the first carbon fiber layer after applying the adhesive resin solution on the first fabric uniformly with the help of a brush. To have a uniform thickness of laminates and avoid epoxy starvation between the two carbon layers, the extra amount of resins were squeezed with the help of a roller onto the carbon fiber woven sheets. The third layer was kept (at 45°/-45° orientation) on the second layer and the same procedure was followed. The 4th, 5th and 6th layers were kept at 45°/-45°, -45°/45° and 90°/0°, respectively in the same manner and the same procedure was adopted towards the preparation of twelve layers of symmetric cross-plied quasi-isotropic CFRP Laminate as shown in Fig. 1. After laying the twelfth layer, peel ply has to be kept and an aluminum plate has to be kept on the top. The carbon fiber/epoxy laminate staking sequence along with fiber orientation and thickness is shown in Fig. 1. During the manufacturing of the CFRPs, the vacuum Bagging Technique was used for curing the whole stack of laminate. In this Vacuum Bagging arrangement, first a mild steel plate was taken and cleaned thoroughly with MEK which was used to form the mould base. After treating this plate with a mould release agent, for making the mould frame Tacky tape was used, with inlet and outlet tubes. The thickness of the laminates fabricated in this entire process was between 3 to 3.5 mm, which meets standard testing requirements.

During this process in order to address air entrapment and void formation the laminate was cured at full vacuum (10 bar). The laminate was kept in this condition for 24 h curing at room temperature. Post curing, laminate was again cured for 1 h at 60 °C and then again at a higher temperature of 120 °C for 3 h. A similar procedure was adopted for the fabrication of other CFRP laminates with different ADG-NH_2/epoxy wt. % (0.25, 0.5, 0.75, and 1). The average thickness of various fabricated ADG-NH_2/epoxy/CFRP composite laminates were 3.02, 3.12, 3.23, 3.34, 3.45 mm respectively for neat, 0.25, 0.5, 0.75 and 1 wt. % ADG-NH_2/epoxy. It was observed that due to the increasing addition of ADG-NH_2 loading content, the average thickness of fabricated CFRP composite laminate increases minimally. For mechanical and morphological characterization, composites were cut into test specimens by means of a high-speed diamond cutter as per the testing standard requirements. The same fabrication technique and identical conditions were adopted for all neat epoxy resin base laminates to compare the performance of graphene content addition.

Methodology of characterization study

Morphology study of ADG-NH_2

In order to evaluate the characteristics of Amine functionalized graphene (ADG-NH_2) nano characterization methodologies such as Fourier transform infrared (FTIR) and scanning electron microscopy (SEM) were carried out. FTIR spectra of the ADG-NH_2 were carried out

using a Hoverlab FT-IR spectrophotometer (model No. HV-5500) with a 2 cm^{-1} resolution over 64 scans. The surface was checked by using a SEM (ZEISS Microscopy, Germany, (Model EVO 15) with a 20 kV acceleration voltage of and 2.5 mm working distance.

The morphology study of the cured ADG-NH_2 enhanced CFRP composites

For this characterization, fracture surfaces were gold coated, and images were studied using a SEM. In order to enhance contrast, a thin gold layer of thickness ~ 3 nm was applied on the fracture surface of the ADG-NH_2 / CFRP composite specimen. X-ray diffraction (XRD) measurements were done with the help of a Siemens D5000 diffractometer along with a Cu-Kα X-ray tube beam radiation (λ = 0.1542 nm) operated at 40 KV and 40 mA. The X-ray diffraction patterns were scanned with the help of a Nickel filter and divergences slits of 1 mm under standard braggs angle θ-2θ conditions. The patterns were scanned over the Bragg angle (2θ) from 1 to 30 ° at a rate of 1°/50 sec^{-1}.

Thermal gravimetric analysis

Thermal gravimetric analysis (TGA) was carried out as per the international standard ISO 11358-1 [31] at a heating rate of 10 °C/min under a nitrogen atmosphere to find the thermal stability of modified composites [32]. From the TGA thermograms, various thermal stability factors such as activation energy (E_t) for decomposition, integral procedural decomposition temperature (IPDT), initial polymer decomposition temperature (PDT) and char yield at 800 °C were determined [33]. IPDT, which indicates the thermal stability of the polymeric materials in the degraded process, was estimated from the TGA curves using the following equations:

$$\mathrm{IPDT} = A^*K^*\left(\theta_f - \theta_i\right) + \theta_i, \quad (1)$$

$$A^* = \frac{A_1+A_2}{A_1+A_2+A_3}, \quad (2)$$

$$K^* = \frac{A_1+A_2}{A_1}, \quad (3)$$

where A^* is the ratio of the total experimental curve defined by the total TGA thermograms, K^* is the coefficient of A^*, θ_i and θ_f are the total initial and final experimental temperatures respectively and A_1, A_2 and A_3 are the areas of the three regions into which the TGA curve is divided as shown in Fig. 2.

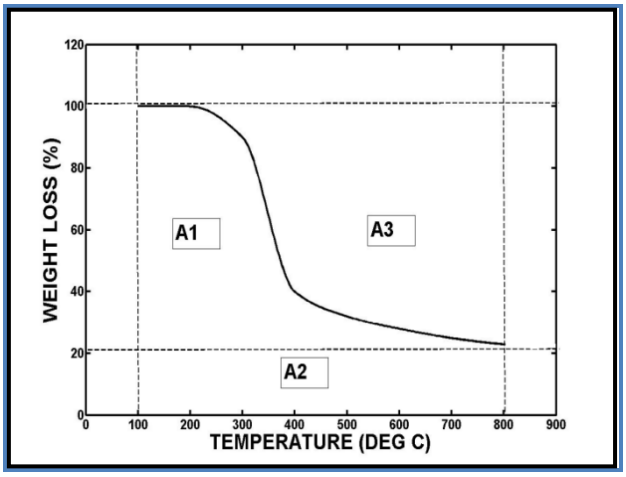

Fig. 2: Schematic representation of A1, A2 and A3

E_t was calculated from the TGA curves using the integral method reported by Horowitz and Metzger, according to the following equations [34]:

$$\ln[\ln(1-\varphi)^{-1}] = \frac{E_t \alpha}{R\theta^2_{\max}} \quad (4)$$

$$\varphi = \frac{(M_i - M_a)}{(M_i - M_f)} \quad (5)$$

$$\alpha = \theta - \theta_{max} \quad (6)$$

where φ is the extent of decomposition, M_a, M_i and M_f are actual, initial and final masses of the sample respectively, R is the universal gas constant, θ_{max} is the absolute temperature.

Dynamic mechanical analysis

Dynamic mechanical analysis (DMA) can identify critical thermal transitions in CFRPs, such as glass transition temperature (T_g) and secondary transitions. T_g is the range of temperatures at which the polymer matrix transitions from a rigid, glassy state to a more flexible, rubbery state. Determining the composite's operational temperature limits requires an understanding of T_g. While, secondary transitions, which can affect the performance of the composite in different environmental conditions. The PerkinElmer DMA 8000(part no N5330101) machine with strain rate of 0.40 and operating at 2 Hz with a temperature range of 400 to -190 °C was used to determine T_g of the modified ADG-NH_2/CFRP composites through DMA. T_g measurements were taken from the maximum values of the tan δ curve. Rectangular specimens of dimensions 3 × 12 × 60 mm^3 were used as per the ASTM D7028 standard [33]. The temperature variation from 30 to 200 °C with an increment of 2 °C/min was carried out on samples. To have repeatability of material response test was carried out on three specimens of each ADG-NH_2/ epoxy wt. % content.

By using Eq. (3), the cross-link density of the ADG-NH_2/epoxy composite with various wt. % concentrations can be found:

$$\rho = \frac{E'}{3RT}, \quad (7)$$

where ρ is cross-link density in mol/cm^3, E' refers to the storage modulus in MPa in the rubbery plateau region, R is the universal gas constant (8.3145 J/K mol), and T is the temperature in rubbery plateau region in Kelvin at T_g + 50.

Results and Discussion

Morphology study of ADG-NH_2

FTIR analysis of the ADG-NH_2 as received was carried out to detect functional groups and characterize covalent bonding information as shown in Fig. 3. Micrograph analysis through SEM for the as received ADG-NH_2 with the higher magnification image was carried out as shown in Fig. 4. The average lateral dimensions of the functionalized graphene particles were found to be of the order of 5 to 10 μm.

Thermal gravimetric analysis

Figure 5 represents the various zones of the TGA theromographs of ADG-NH_2/epoxy/CFRP composite (a) weight loss (%) vs temperature (°C), (b) derivative weight loss (%/min) vs temperature (°C).

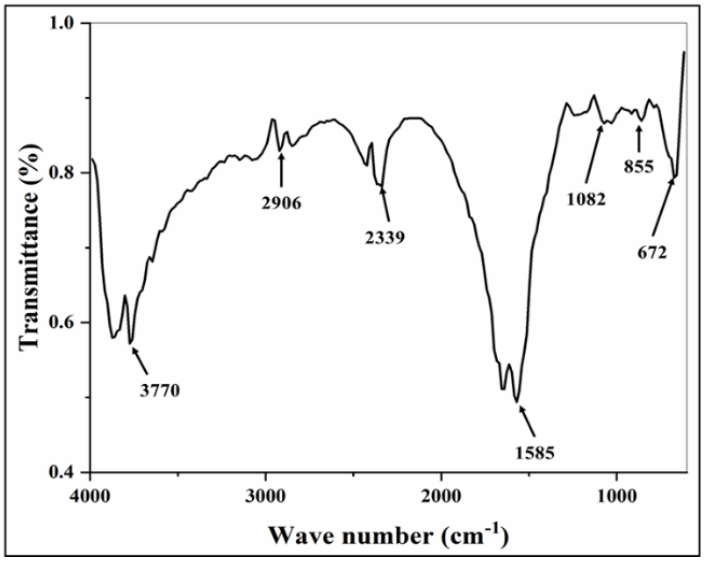

Fig. 3. FTIR spectroscopy of amine functionalized graphene (ADG-NH_2)

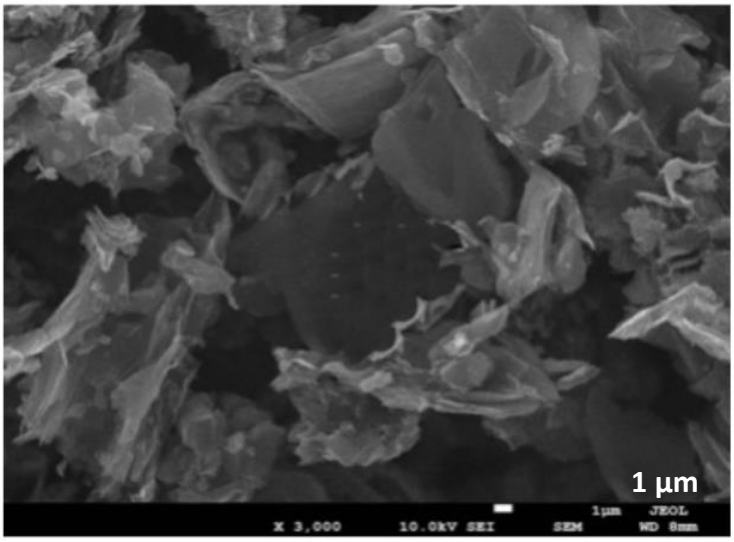

Fig. 4. SEM image of amine functionalized Graphene (ADG-NH_2)

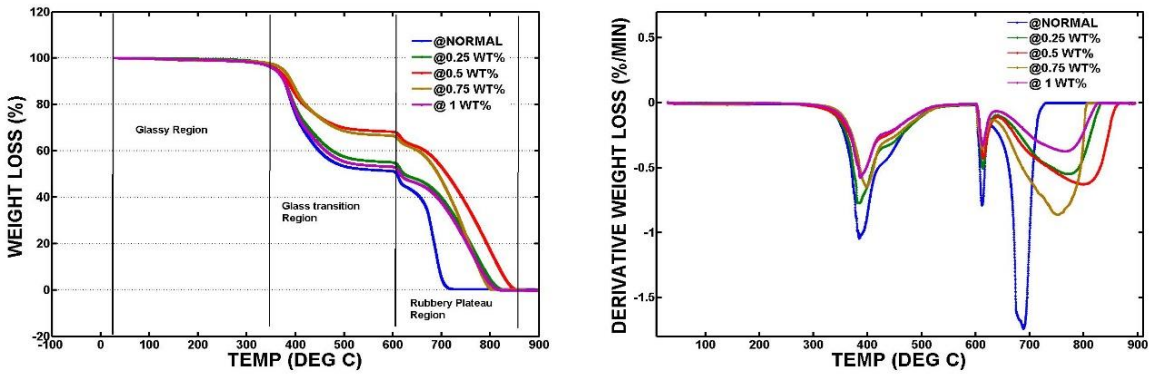

(a) (b)

Fig. 5. TGA theromographs of of ADG-NH_2 /epoxy/ CFRP composite: (a) weight loss (%) Vs temperature (°C), (b) derivative weight loss (%/min) Vs temperature (°C)

As shown in Fig. 5(a), Zone 1 is the glassy region where the first weight loss (10 %) occurs between 25 and 350 °C may be due to the less cured epoxy resin, water vaporisation and volatile impurities. As shown, Zone 2 is the glassy transition region occured between 350 and 600 °C indicating the thermal degradation of the cured epoxy. Figure 5(b) represents the derivative weight loss (%/min) vs temperature (°C) for different wt. % of graphene fillers.

The thermal stability factors, including PDT, IPDT, E_t and Char yield at 800 °C are listed in Table 1. The PDT and IPDT values of the ADG-NH_2/epoxy/CFRP composites were 362.59 and 389.1 °C, respectively. The maximum PDT and IPDT values were observed as 373.02 and 411.9 °C, respectively, occurred at 0.5 wt. % ADG-NH_2 content. An increase of ~ 14 % was observed for the activation energy (E_t) values of the modified composites, which were increased from 61.63 to 69.93 KJ mol^{-1} as listed in Table 1.

Table 1. PDT, IPDT, E_t and char yield at 800 °C values observed from TGA thermograms

ADG-NH_2 loading, wt. %	PDT, °C	IPDT, °C	E_t, KJ/mol	Char yield at 800 °C
0	362.59	389.1	61.63	0.43
0.25	364.30	394.8	65.52	2.58
0.5	373.02	411.9	69.93	4.55
0.75	367.11	406.2	68.098	0.32
1.0	363.11	400.5	64.95	0.24

Also, an increase in characteristic yields of the prepared composites at 800 °C was observed for 0.5 wt. % ADG-NH_2 content compared to neat epoxy and reduces subsequently beyond 0.5 wt. %. These results indicate improved thermal stability characteristics such as thermal resistance and thermal conductivity of the polymer structure due to the addition of ADG-NH_2 graphene fillers of up to 0.5 wt. % compared to neat epoxy. Beyond 0.5 wt. % ADG-NH_2 graphene fillers, there is an agglomeration formation in the epoxy network which reduces the interfacial bonding characteristics of the fiber epoxy network [33–35].

Dynamic mechanical properties

DMA uses modulus and tan δ to quantify the sample's stiffness and damping. Since the applied force is sinusoidal, the storage modulus (E') can be expressed as an in-phase component and loss modulus (E'') an out-of-phase component. The elastic response of the sample is represented by the E', and the capacity to dissipate energy is represented by tan δ (i.e. E''/E'). This analysis quantifies the loss modulus (E''), storage modulus (E'), damping factor (tan δ), and glass transition temperature (T_g). Figure 6 represents the viscoelastic properties of ADG-NH_2/epoxy/CFRP composites w.r.t temperature for different wt. % of ADG-NH_2 filler investigated through dynamic mechanical analysis.

Figure 6(a) represents the storage modulus (E') vs temperature of modified composites at different wt. % of ADG-NH_2. These curves depict the three significant zones

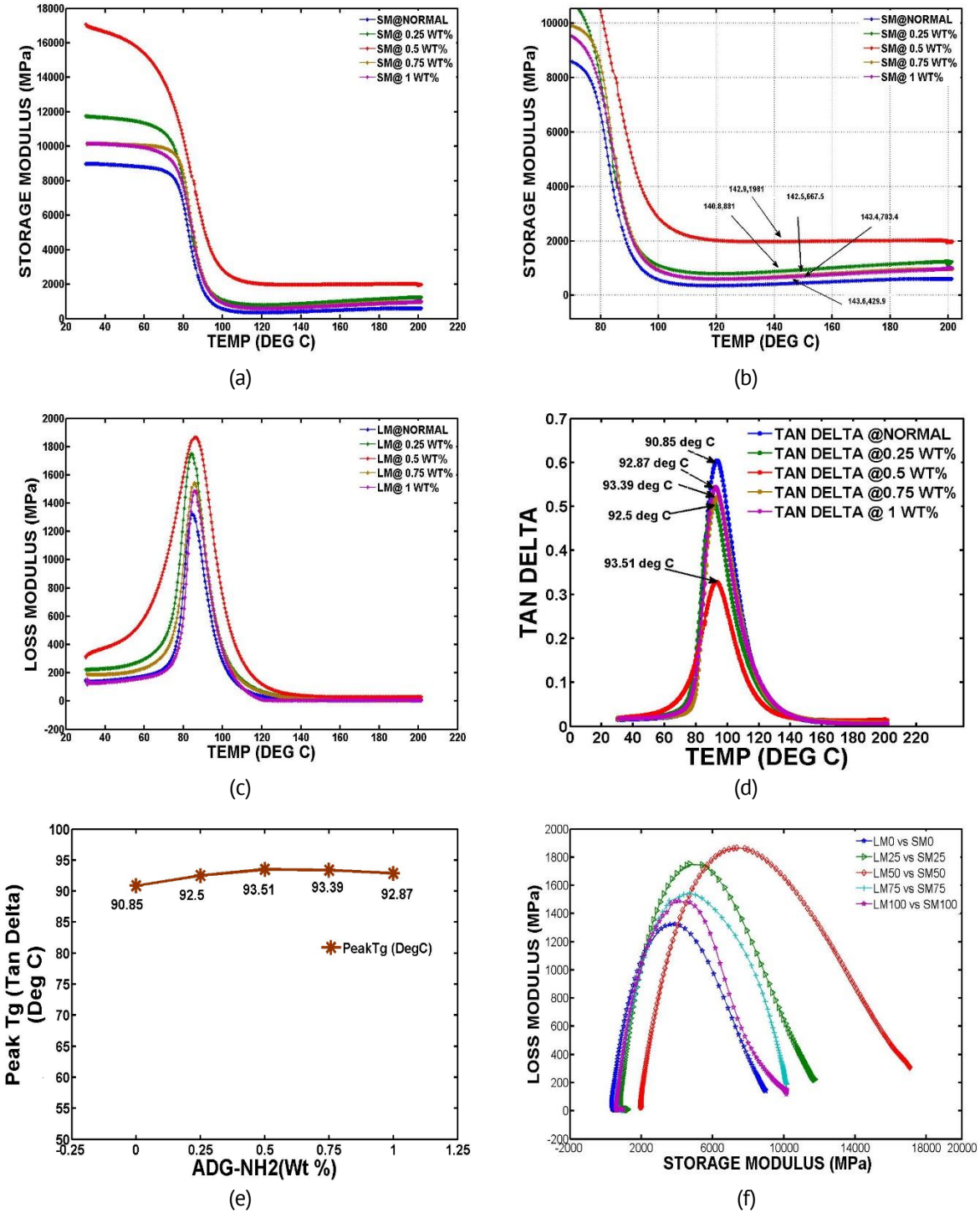

Fig. 6. Variation of (a) storage modulus vs temperature, (b) storage modulus (rescale showing T_g+50) vs temperature,(c) loss modulus vs temperature, (d) tan δ Vs temperature, (e) peak T_g w.r.t ADG-NH_2 addittion, (f) Cole-Cole plots of ADG-NH_2/epoxy/CFRP composites

of the material during the experiment, such as the glassy region (Zone 1) representing the elasticity, the rubbery transition region (Zone 2) which indicates the degradation of and decreases beyond 0.5 wt. %.

Due to the hexagonal molecular arrangement of graphene with carbon fiber atomic structure, semi compatibilty local agglomerations elasticity till it stabilizes and enters the

rubbery region (Zone 3). At 65–75 °C for all curves there is a sudden decreasing trend in all the curves indicating the end stage of the glassy region of the CFRP composite. Table 2 lists the maximum storage modulus values of the ADG-NH_2/epoxy/CFRP composite based on the experiments on the different wt. % of ADG-NH_2 in CFRP composites. As the ADG-NH_2 graphene concentration increases, *E'* of modified composites increased to 10325 MPa (for 0.25 wt. %), 12872 MPa (for 0.5 wt. %), 9723MPa (0.75 wt. %), 9150 MPa (1 wt. %) respectively from 8346 MPa (Neat CFRP) which corresponds to increment of 23.71, 54.22, 16.5 and 9.6 % respectively. It can be concluded from the above observations that the storage modulus increased up to 0.5 wt. % of ADG-NH_2 were formed beyond 0.5 wt. % which prevents higher elastic behavior for the rubbery transition zone across the full temperature range [36–39].

Table 2. Maximum storage modulus and loss modulus observed during the DMA of ADG-NH_2/epoxy/CFRP composite specimens

ADG-NH_2 loading, wt. %	Max storage modulus (*E'*), MPa	Increase in *E'*, %	Max loss modulus *E''*, MPa	Increase in *E''*, %
Neat epoxy	8346 + 41.53	0	1324 + 13.24	0
0.25	10325 + 51.63	23.71	1750 + 17.5	32.17
0.5	12872 + 64.36	54.22	1866 + 18.66	40.93
0.75	9723 + 48.62	16.5	1545 + 15.45	16.69
1	9150 + 45.75	9.6	1487 + 14.87	12.31

Figure 6(b) represents the enlarged view of storage modulus (*E'*) values of modified composites at a temperature of T_g+ 50 where the cross-link density, values are estimated for different wt. % of ADG-NH_2. Table 3 lists the cross-link density values of the modified CFRP composite using Eq. (3). The cross-link density which indicates the stiffness characteristics of the polymer structure is affected by the mobility of molecules in the polymeric chain. Its value increased up to 0.5 wt. % of ADG-NH_2 and subsequently reduced beyond 0.5 wt. %.

Table 3. Peak glass transition (T_g) and peak tg δ of ADG-NH_2 filled CFRP composites

ADG-NH_2 loading, wt. %	Peak T_g, °C (loss peak)	Peak *Tg*, °C (tan δ peak)	Peak tg δ	Cross link density, mol/cm^3
Neat epoxy	84.24 + 0.22	90.85 + 0.25	0.6041	0.041
0.25	84.39 + 0.25	92.5 + 0.32	0.5202	0.085
0.5	86.08 + 0.35	93.51 + 0.35	0.3284	0.191
0.75	85.72 + 0.33	93.39 + 0.33	0.5144	0.068
1	85.65 + 0.30	92.87 + 0.30	0.544	0.064

The reduction in the T_g value listed in Table 3 indicates the decrease in stiffness value of the composite material. The storage modulus values are directly related to highly cross-linked polymeric chain and vice versa [40,41].

Figure 6(c) represents the loss modulus (*E''*) vs temperature of modified composites at different wt. % of ADG-NH_2, which indicates the energy release by the polymer structure when subjected to cyclic loading. As illustrated in these curves the values initially increase in zone 1 i.e. glassy region and then sharply increases to the peak in Zone 2 i.e. Rubbery transition zone but sharply reduces in this region and continues up

to Zone 3 Rubbery region. It was observed that the loss modulus of approx. 41 % increased up to 0.5 wt. % of ADG-NH_2 and decreased beyond 0.5 wt. %. The inclusion of ADG-NH_2 frequently causes the loss modulus peak to broaden. This phenomenon is typically attributed to either a suppression of the relaxation process occurring inside the composite or a higher rigidity of the chain segments, hence increasing the material's heterogeneity. In the ADG-NH_2-loaded samples, the loss modulus was essentially increased for three reasons: (1) the polymer chains were unable to move freely as a result of the amino-functionalized GNP's enhancement of the crosslinking reactions between epoxy and hardener; (2) the covalent bond formed between the amino-functionalized GNP and epoxy enabled greater energy dissipation from the matrix to the amino-functionalized GNP, and (3) demonstrating the enhanced adhesion and interfacial bonding strength between the resin matrix and carbon fiber. The addition of amino functionalized GNP raises the composites' loss modulus (E'') in comparison to the untreated composite, which in turn raises the polymer's structural mobility inside the composite. The polymer chain relaxation zones and confluence zones were observed for all the curves towards the peak loss modulus values, but relaxation zones were more for the more ADG-NH_2 graphene loading content beyond 0.5 wt. %. Peak E'' was measured at 1324, 1750, 1866, 1545 and 1487 MPa at 84.39, 84.72, 86.69, 85.33 and 85.28 °C. The increase in loss modulus values up to 0.5 wt. %, which represents the better energy dissipation and mechanical properties was may be due to the better graphene dispersion, enhancement of the cross-linking reactions between epoxy and hardener, greater energy dissipation from the matrix to the amino-functionalized GNP and enhanced fiber matrix bonding [32,42].

Figure 6(d) represents tan δ vs temperature of modified composites at different wt. % of ADG-NH_2 which indicates the damping properties as well as the material characteristics whether it is elastic or non-elastic in nature for the polymer structure. A material with a high, non-elastic strain component is indicated by a high tan δ value, whereas a low value denotes a material with high elasticity. The damping factor is governed by molecular motions and viscoelasticity, in addition to specific defects that promote damping, are dislocations, grain boundaries, phase barriers, and different interfaces. The damping factor is reduced with an increase in the bonding at the fiber/matrix interaction because of decreased mobility of the molecular chains at the fiber/matrix interface. Thus, the higher the energy losses with respect to its storage capacity, the greater will be the tan δ value in the composite system [43,44]. As depicted from the curves, tan δ values obtained for different wt. % fillers are 0.6041, 0.5202, 0.3284, 0.5144, 0.544 respectively for neat CFRP, 0.25, 0.5, 0.75 and 1 wt. % as listed in Table 3. The peak T_g values for all Tan δ values are shown in Fig. 6(d) and are listed in Table 3. It was observed that the peak of all the tan δ values decreased with an increase in ADG-NH_2 filler content. The minimum value obtained for 0.5 wt. % represents more elasticity characteristics and better interfacial bonding compared to the maximum value obtained for neat epoxy representing better damping , energy dissipation and weak interfacial bonding between fiber and matrix interfaces [45–47].

Figure 6(e) represents the peak T_g values for different ADG/NH_2 concentrations of the CFRP matrix. The glass transition temperature T_g is defined as the temperature where (i) the middle point of E' vs. temperature curve or (ii) the region where E' increases with

increasing frequency at constant temperature or (iii) maximum of *E*" happens or (iv) maximum of tan δ arises. It was observed that a very slight increment in T_g up to 0.5 % addition of ADG/NH_2, thereafter decrement was observed.

Figure 6(f) represents the relation between the loss modulus indicating the viscoelastic material energy dissipation and storage modulus indicating the stored energy of the polymer material known as the Cole-Cole plot. These plots indicate the homogenity or hetrogenity characteristics of material w.r.t different wt. % of graphene fillers and information about the structural rigidness at high temperatures. As observed, all the curves of the composite were of a warped semicircular contour indicating their heterogeneous characteristics [48,49]. Due to localized agglomeration of the graphene particles for higher wt. % beyond 0.5, curves were displayed as imperfect semicircles indicating the viscoelastic behavior of the polymer structure [50,51].

Figure 7(a) represents the relationship between the cross-link density w.r.t ADG-NH_2 wt. %. Figure 7(b) represents the relationship between FWHM (full width at half maximum) of loss modulus w.r.t ADG-NH_2 wt. %. In both the grphs it was observed that the values are increased up to 0.5 wt. % and reduced subsequently beyond 0.5 wt. %.

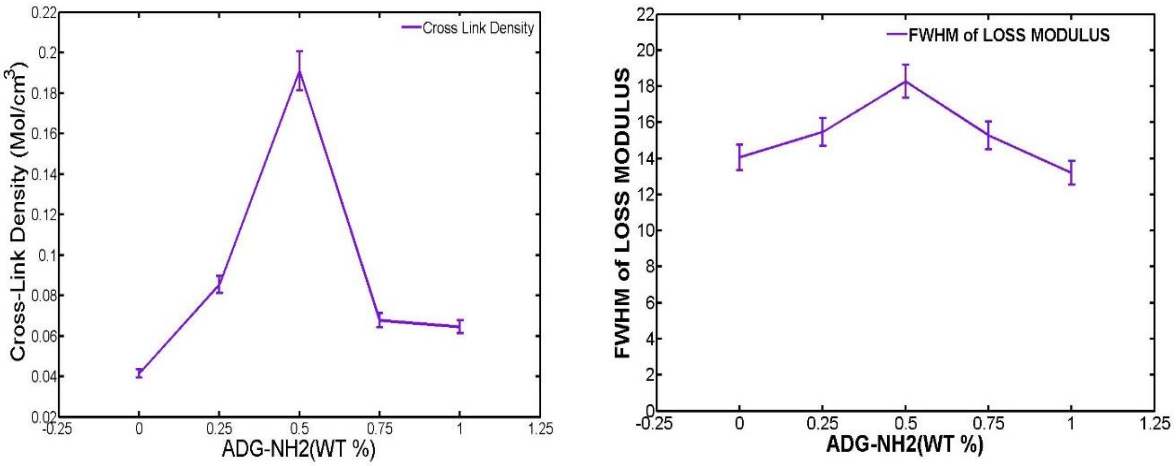

(a) (b)

Fig. 7. Variation of (a) cross link densty Vs ADG-NH_2 filler loading corelation, (b) FWHM of loss modulus Vs ADG-NH_2 filler loading corelation

Fractographic analysis of ADG-NH_2/CFRP

SEM micrograph and XRD analysis were carried out to evaluate the physical and chemical properties along with the toughening mechanism of the ADG-NH_2 nano material for both neat epoxy and ADG-NH_2/ CFRP with different wt. % filler content (0.25, 0.5, 0.75 and 1) (Fig. 8). Neat and ADG-NH_2/CFRP composites epoxy with varying filler levels (0.25, 0.5, 0.75, and 1 wt. %) were examined using SEM examination. The fracture toughness of CFRP laminate is determined by the toughness of the matrix and adherence of the carbon fibers to the matrix. Amine-functionalized graphene increases fracture toughness, because of its mechanical strength, surface area, wrinkled structure, and good interfacial adhesion with epoxy. The amine groups improve bonding with the epoxy matrix, also aiding uniform dispersion of graphene. At higher concentrations (0.75 and 1 wt. %), graphene aggregation causes stress concentration and reduced adhesion, negatively

impacting performance. SEM images confirm uniform dispersion in lower concentrations but show exposed fibers and poor bonding at 1 wt. %, explaining the decline in mechanical performance at higher filler contents.

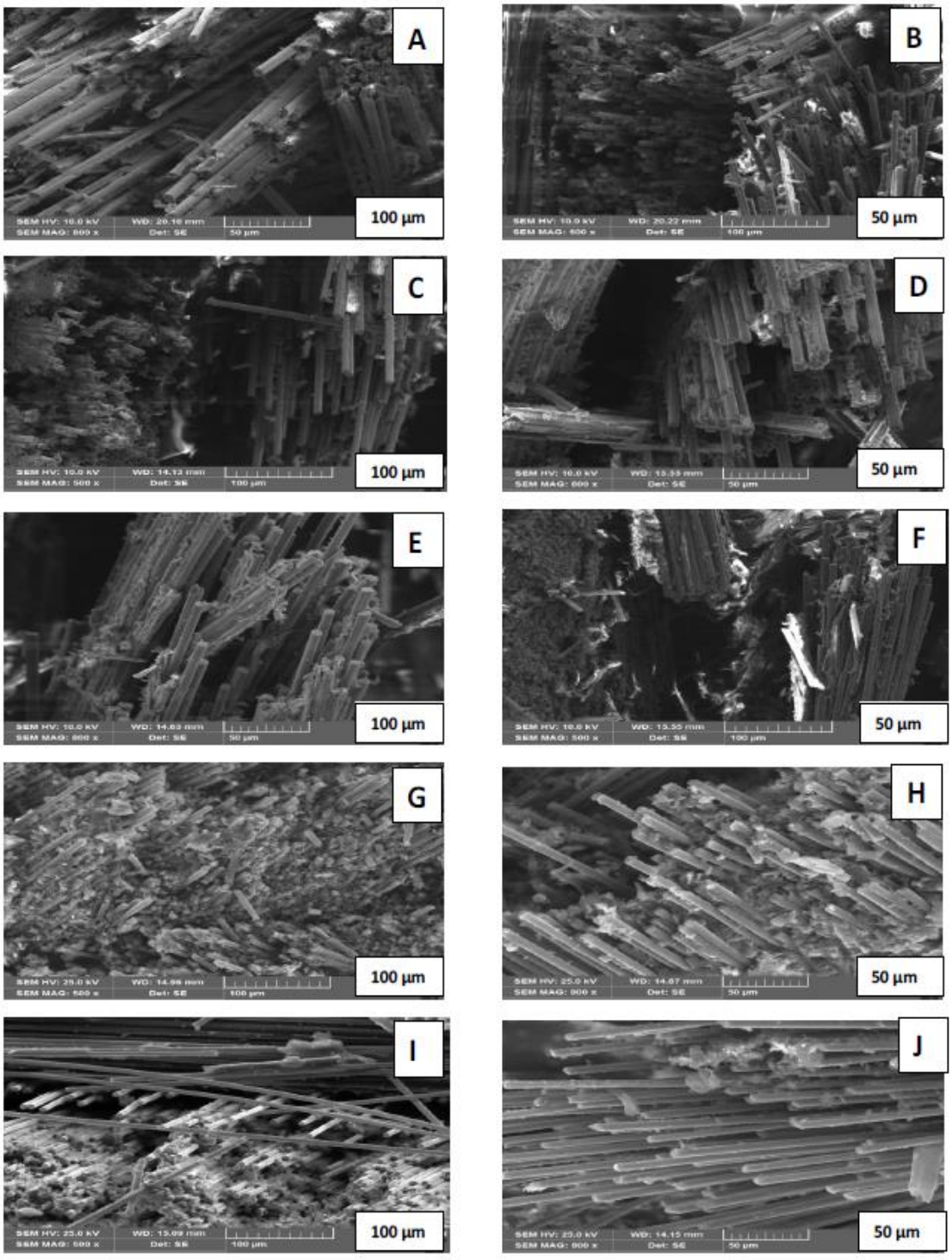

Fig. 8. SEM images of (A,B) CFRP with neat epoxy (100 µm) & (50 µm), (C,D) CFRP with 0.25 wt. % of graphene (100 µm) & (50 µm), (E,F) CFRP with 0.5 wt. % of graphene (100 µm) &(50 µm), (G,H) CFRP with 0.75 wt. % of graphene (100 µm) & (50 µm), (I,J) CFRP with 1 wt. % of graphene (100 µm) & (50 µm)

SEM pictures show weak mechanical properties due to brittle fracture behavior, exposed carbon fibers, and poor bonding in neat epoxy matrix. In contrast, amine-functionalized graphene strengthens adhesion, as demonstrated by the firmly bonded carbon fibers in matrix material. As shown in Fig. 8(e,f), fractured samples with 0.5 wt. %, graphene exhibits the best interfacial strength and rough fracture surfaces, indicating plastic deformation and crack deflection. Increased surface area and energy absorption during fracture propagation are indicated by dimples, which enhance mechanical characteristics. Performance is adversely affected by graphene aggregation at higher concentrations (0.75 and 1 wt. %), which results in stress concentration and decreased adhesion in Fig. 8(g,h,I,j). The decrease in mechanical performance at increasing filler amounts can be explained by SEM images, which show exposed fibers and weak bonding at 1 wt. % but demonstrate homogeneous dispersion at lower concentrations.

X-ray diffraction (XRD) analysis was carried out on the ADG-NH_2/CFRP composite laminate to evaluate the crystallinity and interlayer distance of the nano materials. The XRD image pattern for the neat epoxy CFRP indicates that the primary peak (002) was observed at ~ 24.89°, which represents an interlayer distance of ~ 0.357 nm, along with the (004) peak occurring at 44.60°. The XRD image pattern for ADG-NH_2/CFRP composite laminates with different wt. % filler content (0.25, 0.5, 0.75 and 1) indicates the primary

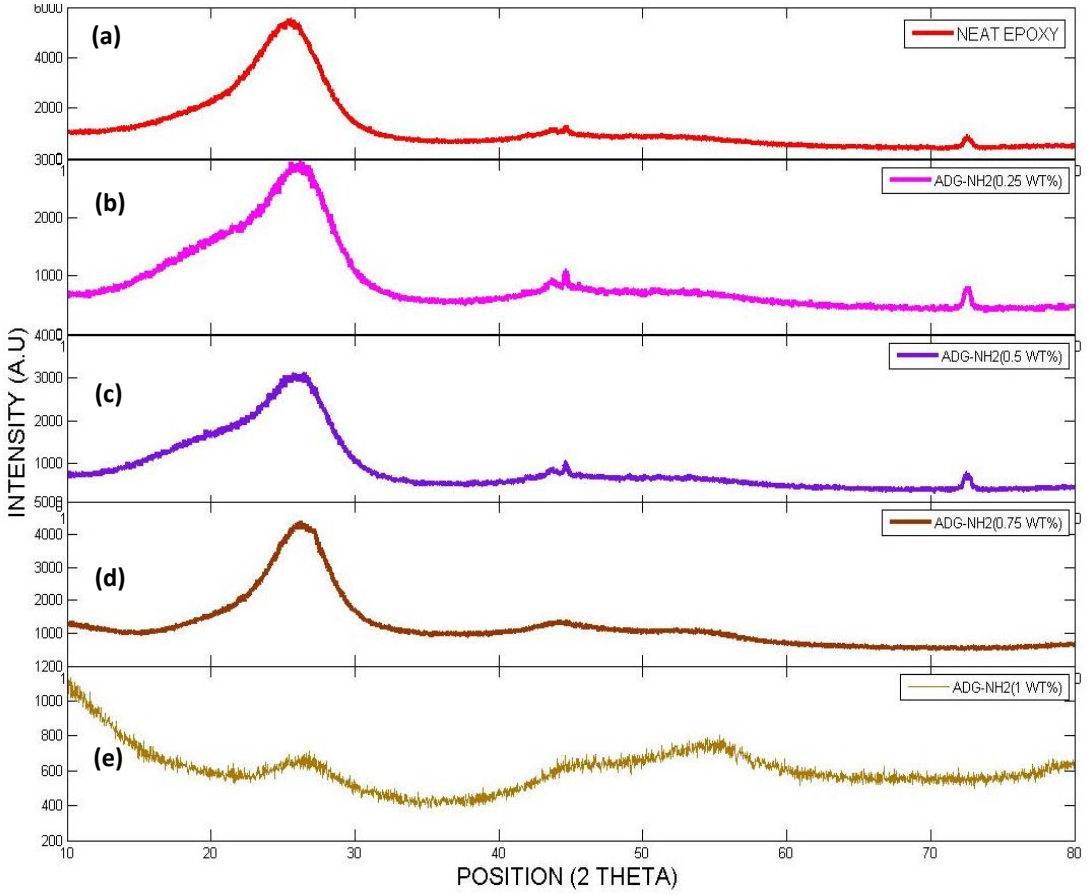

Fig. 9. XRD patterns of (a) CFRP with neat epoxy with peak 2θ =24.89°, (b) CFRP with 0.25 wt. % of graphene with peak 2θ =26.80°, (c) CFRP with 0.5 wt. % of graphene with peak 2θ =26.65°, (d) CFRP with 0.75 wt. % of graphene with peak 2θ =26.90°, (e) CFRP with 1 wt. % of graphene with peak 2θ =25.78°

(002) peak were present at ~ 26.80, ~ 26.65, ~ 26.90, ~ 25.78° respectively which corresponds to an interlayer distance of ~ 0.332, ~ 0.334, ~ 0.331, ~ 0.334 nm, respectively (Fig. 9). These XRD patterns indicate that the impurities or enormous amounts of dislocated or corrugated carbon samples are not available in the composite laminates. These diffraction patterns of the profile peaks also indicate the high degree of crystallinity in the composite laminates.

Conclusions

In order to evaluate the effect of Amine functionalized graphene (ADG-NH_2) reinforced CFRP composites on thermal properties, various specimens of different wt. % have been prepared as per ASTM requirements. The fractographic study indicates encouraging thermal properties due to an improved adhesion mechanism influenced by the homogenous dispersion of amine functionalization of graphene (ADG-NH_2).

The results of thermal characterization of modified composites evaluated through DMA reveal that an increase of ~ 55 and ~ 41 % was observed for the storage modulus and loss modulus at 0.5 wt. % of ADG-NH_2 graphene content compared to the neat epoxy, CFRP composites indicating better elasticity, viscoelastic properties and energy dissipation capabilities. The minimum tan delta values were obtained for 0.5 wt. % of ADG-NH_2 graphene content compared to neat epoxy indicating better damping , energy dissipation and superior interfacial bonding between fiber and matrix interfaces. As observed from the loss modulus curves and tan δ curves the T_g values were also observed to be improved by ~ 2 % compared to neat epoxy CFRP. Fractographic analysis from SEM and XRD clearly demonstrates the improvement of layer adhesion for increasing loading content up to compared to neat epoxy CFRP. This work demonstrates the distinct enhancements in thermal properties of laminates compared to previous results due to homogeneous dispersion of GNP in ADG-NH_2-epoxy CFRP composite and better load transfer in nanomaterial.

CRediT authorship contribution statement

Debendra Nath Choudhury: conceptualization, methodology, software, data curation, formal analysis, visualization, validation, writing—original draft preparation, resources, writing—review and editing, funding acquisition; **Saroja Kanta Panda**: software, visualization, validation, resources, investigation, writing—review and editing, supervision, project administration.

Conflict of interest

The authors declare that they have no conflict of interest.

References

1. Chiou YC, Chou HY, Shen MY. Effects of adding graphene nano platelets and nano carbon aerogels to epoxy resins and their carbon fiber composites. *Materials & Design.* 2019;178: 107869.
2. Bhanuprakash L, Parasuram S, Varghese S. Experimental investigation on graphene oxides coated carbon fibre /epoxy hybrid composites: Mechanical and electrical properties. *Composites Science and Technology.* 2019;179: 134–144.

3. Sayam A, Rahman ANMM, Rahman MS, Smriti SA, Ahmed F, Rabbi MF, Hossain M, Faruque MO. A review on carbon fiber-reinforced hierarchical composites: Mechanical performance, manufacturing process, structural applications and allied challenges. *Carbon Letters*. 2022;32(5): 1173–1205.
4. Ou Y, González C, Vilatela JJ. Interlaminar toughening in structural carbon fiber / epoxy composites interleaved with carbon nanotube veils. *Composites Part A: Applied Science and Manufacturing*. 2019;124: 105477.
5. Li N, Wang GD, Melly SK, Peng T, Li YC, Zhao QD, Ji SD. Interlaminar properties of GFRP laminates toughened by CNTs bucky paper interlayer. *Composite Structures*, 2019;208: 13–22.
6. Ackermann C, Demleitner M, Guhathakurta J, Carosella S, Ruckdäschel H, Simon S, Middendorf P. Mechanical, thermal, and electrical properties of amine-and non-functionalized reduced graphene oxide/epoxy carbon fiber-reinforced polymers. *Polymer Composites*. 2023;44(8): 4937–4954.
7. Raj MKA, Muthusamy S, Panchal H, Ibrahim AMM, Alsoufi MS, Elsheikh AH. Investigation of mechanical properties of dual-fiber reinforcement in polymer composite. *Journal of Materials Research and Technology*. 2022;18: 3908–3915.
8. Burger N, Laachachi A, Ferriol M, Lutz M, Toniazzo V, Ruch D. Review of thermal conductivity in composites: Mechanisms, parameters and theory. *Progress in Polymer Science*. 2016;61: 1–28.
9. Ma J, Q Meng, I Zaman, S Zhu, A Michelmore, N Kawashima, CH Wang, HC Kuan, Development of polymer composites using modified, high-structural integrity graphene platelets. *Composites Science and Technology*. 2014;91: 82–90.
10. Ahmadi-Moghadam B, Sharafimasooleh M, Shadlou S, Taheri F. Effect of functionalization of graphene nanoplatelets on the mechanical response of graphene/epoxy composites. *Materials & Design (1980-2015)*. 2015;66: 142–149.
11. Fang H, Bai SL, Wong CP. Microstructure engineering of graphene towards highly thermal conductive composites. *Composites Part A: Applied Science and Manufacturing*. 2018;112: 216–238.
12. Shen L, Zhang X, Lei Y, Liang M, Chen Y, Chen W, Zou H. Efficient reinforcement of epoxy resin with amine-rich rigid short-chain grafted graphene oxide. *Polymer Composites*. 2021;42(9): 4775–4785.
13. Cai Z, Meng X, Han Y, Ye H, Cui L, Zhou Q. Reinforcing polyamide 1212 with graphene oxide via a two-step melts compounding process. *Composites Part A: Applied Science and Manufacturing*. 2015;69: 115–123.
14. Li Y, Zhang H, Porwal H, Huang Z, Bilotti E, Peijs T. Mechanical, electrical and thermal properties of in-situ exfoliated graphene/epoxy nano composites. *Composites Part A: Applied Science and Manufacturing*. 2017;95: 229–236.
15. Chee SS, Jawaid M, Sultan MTH, Alothman OY, Abdullah LC. Thermo mechanical and dynamic mechanical properties of bamboo/woven kenaf mat reinforced epoxy hybrid composites. *Composites Part B: Engineering*. 2019;163: 165–174.
16. Costa C, Fonseca AC, Serra AC, Coelho JFJ. Dynamic mechanical thermal analysis of polymer composites reinforced with natural fibers. *Polymer Reviews*. 2016;56(2): 362–383.
17. Md Shah AU, Sultan MTH, Jawaid M. Sandwich-structured bamboo powder/glass fibre-reinforced epoxy hybrid composites-Mechanical performance in static and dynamic evaluations. *Journal of Sandwich Structures & Materials*. 2021;23(1): 47–64.
18. Saba N, Jawaid M, Alothman OY, Paridah MT. A review on dynamic mechanical properties of natural fibre reinforced polymer composites. *Construction and Building Materials*. 2016;106: 149–159.
19. Zeki C, Gardner DJ, Shaler SM. Dynamic mechanical thermal analysis (DMTA) of cellulose nano fibril / nano clay / pMDI nano composites. *Composites Part B. Engineering*. 2016;90: 126–132.
20. Saba N, Safwan A, Sanyang ML, Mohammad F, Pervaiz M, Jawaid M, Alothman OY, Sain M. Thermal and dynamic mechanical properties of cellulose nano fibers reinforced epoxy composites. *International Journal of Biological Macromolecules*. 2017;102: 822–828.
21. Atiqah A, Jawaid M, Sapuan SM, Ishak MR, Alothman OY. Thermal properties of sugar palm/glass fiber reinforced thermoplastic polyurethane hybrid composites. *Composite Structures*. 2018;202: 954–958.
22. Gupta A, Hasanov S, Fidan I. Thermal characterization of short carbon fiber reinforced high temperature polymer material produced using the fused filament fabrication process. *Journal of Manufacturing Processes*. 2022;80: 515–528.
23. Yadav A, Kumar A, Singh PK, Sharma K. Glass transition temperature of functionalized graphene epoxy composites using molecular dynamics simulation. *Integrated Ferroelectrics*. 2018;186(1): 106–114.
24. Kumar A, Sharma K, Dixit AR. Carbon nanotube-and graphene-reinforced multiphase polymeric composites: review on their properties and applications. *Journal of Materials Science*. 2020;55(7): 2682–2724.
25. Kumar A, Sharma K, Dixit AR. A review of the mechanical and thermal properties of graphene and its hybrid polymer nano composites for structural applications. *Journal of Materials Science*. 2019;54(8): 5992–6026.
26. Jesuarockiam N, Jawaid M, Zainudin ES, Thariq Hameed Sultan M, Yahaya R. Enhanced thermal and dynamic mechanical properties of synthetic/natural hybrid composites with graphene nanoplateletes. *Polymers*. 2019;11(7): 1085.
27. Rashmi BJ, Prashantha K, Lacrampe MF, Krawczak P. Scalable production of multifunctional bio-based polyamide 11/graphene nano composites by melt extrusion processes via masterbatch approach. *Advances in Polymer Technology*. 2018;37(4): 1067–1075.

28. Chinnasamy S, Ramachandran M, Kurinjimalar Ramu PA. Study on fuzzy ELECTRE method with various methodologies. *REST Journal on Emerging trends in Modelling and Manufacturing*. 2022;7(4): 108–115.
29. Choudhury DN, Pareta AS, Rajesh AK, Panda SK. Enhanced mechanical and interfacial performances of carbon fiber reinforced composites with low percentage of amine functionalized graphene. *Polymer Composites*. 2024;45(15): 13772–13790.
30. Choudhury DN, Panda SK. Effect of ADG-NH_2 functionalized graphene on fracture and impact resistance of carbon fiber reinforced composites. To be published in *Res. Eng. Struct. Mat.* [Preprint] 2025. Available from: dx.doi.org/10.17515/resm2025-588me1224rs.
31. International Organization for Standardization. ISO 11358-1:2022. *Plastics Thermogravimetry (TG) of polymers Part 1: General principles*. ISO; 2022.
32. Mushtaq, H. B. Mukhtar, A. M. Shariff. Effect of glass transition temperature in enhanced polymeric blend membranes. *Procedia Engineering*. 2016;148: 11–17.
33. American Society for Testing and Materials. ASTM D7028-07(2015). *Standard Test Method for Glass Transition Temperature (DMA Tg) of Polymer Matrix Composites by Dynamic Mechanical Analysis (DMA)*. West Conshohocken, Pa, USA: ASTM; 2015.
34. Doyle CD. Estimating thermal stability of experimental polymers by empirical thermo gravimetric analysis. *Analytical Chemistry*. 1961;33(1): 77–79.
35. Szeluga U, Kumanek B, Trzebicka B. Synergy in hybrid polymer/nano carbon composites. A review. *Composites Part A: Applied Science and Manufacturing*. 2015;73: 204–231.
36. Yue L, Pircheraghi G, Monemian SA, Manas-Zloczower I. Epoxy composites with carbon nanotubes and graphene nano platelets–Dispersion and synergy effects. *Carbon*. 2014;78: 268–278.
37. Costa C, Fonseca AC, Serra AC, Coelho JFJ. Dynamic Mechanical Thermal Analysis of Polymer Composites Reinforced with Natural Fibers. *Polymer Reviews*. 2016;56(2): 362–383.
38. Chen H, Ginzburg VV, Yang J, Yang Y, Liu W, Huang Y, Du L, Chen B. Thermal conductivity of polymer-based composites: Fundamentals and applications. *Progress in Polymer Science*. 2016;59: 41–85.
39. Hossain MK, Chowdhury MMR, Hosur M, Bolden NW. Viscoelastic Properties of Carbon/Epoxy Amino-Functionalized Graphene Nano platelet Composite. *ASME International Mechanical Engineering Congress and Exposition*. 2016;50633: V009T12A027.
40. Prolongo SG, Gude MR, Ureña A. Improving the flexural and thermo mechanical properties of amino-functionalized carbon nanotube/epoxy composites by using a pre-curing treatment. *Composites Science and Technology*. 2011;71(5): 765–771.
41. Cai Z, Meng X, Han Y, Ye H, Cui L, Zhou Q. Reinforcing polyamide 1212 with graphene oxide via a two-step melt compounding process. *Composites Part A: Applied Science and Manufacturing*. 2015;69: 115–123.
42. Jesuarockiam N, Jawaid M, Zainudin ES, Thariq Hameed Sultan M, Yahaya R. Enhanced thermal and dynamic mechanical properties of synthetic/natural hybrid composites with graphene nano plateletes. *Polymers*. 2019;11(7): 1085.
43. Rasana N, Jayanarayanan K, Deeraj BDS, Joseph K. The thermal degradation and dynamic mechanical properties modeling of MWCNT/glass fiber multiscale filler reinforced polypropylene composites. *Composites Science and Technology*. 2019;169: 249–259.
44. Kang WS, Rhee KY, Park SJ. Thermal, impact and toughness behaviours of expanded graphite/graphite oxide-filled epoxy composites. *Composites Part B: Engineering*. 2016;94: 238–244.
45. Wang J, Ma F, Sun M. Graphene, hexagonal boron nitride, and their hetero structures: properties and applications. *RSC Advances*. 2017;7(27): 16801–16822.
46. Badgayan ND, Sahu SK, Samanta S, Sreekanth PR. Evaluation of dynamic mechanical and thermal behavior of HDPE reinforced with MWCNT/h-BNNP: an attempt to find possible substitute for a metallic knee in transfemoral prosthesis. *International Journal of Thermophysics*. 2019;40: 93.
47. Chee SS, Jawaid M, Sultan MTH, Alothman OY, Abdullah LC. Thermo mechanical and dynamic mechanical properties of bamboo/woven kenaf mat reinforced epoxy hybrid composites. *Composites Part B. Engineering*. 2019;163: 165–174.
48. Li Y, Zhang H, Porwal H, Huang Z, Bilotti E, Peijs T. Mechanical, electrical and thermal properties of in-situ exfoliated graphene/epoxy nano composites. *Composites Part A: Applied Science and Manufacturing*. 2017;95: 229–236.
49. Chandrasekhar GL, Vijayakumar Y, Nagaral M, Rajesh A, Manjunath K, Kaviti RVP, Auradi V. Synthesis and tensile behavior of Al7475-nano B4C particles reinforced composites at elevated temperatures. *Materials Physics and Mechanics*. 2024;52(3): 44–57.
50. Lamba NK. Quasi-static thermal response of a circular plate due to the influence of memory-dependent derivatives. *Materials Physics and Mechanics*. 2024;52(4): 163–172.
51. Pozdnyakov AO, Sedakova EB. Thermal analysis of wear of polymer-polymer friction pairs in vacuum and atmosphere conditions. *Materials Physics and Mechanics*. 2024;52(4): 63–80.